CrossMark

Microstructure and magnetic properties of hot-deformed anisotropic Nd–Fe–B magnets prepared from amorphous precursors with different crystallization proportions

Wei Zhao, Ying Liu, Jun Li* , **Ren-Quan Wang, Yu-Chong Qiu**

Abstract Anisotropic magnets were obtained by hot deformation with the partial crystallized precursor prepared via spark-plasma sintering (SPS). Amorphous powders with the nominal composition of $Nd_{28.72}Fe_{bal}Co_{5.66}Ga_{0.59}B_{0.92}$ (wt%) were used as the starting material. The results show that the amorphous powders would suffer varying degrees of crystallization even below the crystallization point during the SPS process under high pressure. And the pre-crystallized grains in precursors have great impacts on the microstructure and magnetic properties of the hot-deformed magnets. The final obtained anisotropic magnets exhibit homogeneous microstructure consisting of well-aligned and platelet-shaped $Nd_2Fe_{14}B$ grains without abnormal growth. It can be found that a reasonable proportion of pre-crystallized gains could promote the preferential orientation in the magnet, leading to the achievement of optimal magnetic properties among the magnets with identical composition and best magnetic performance is achieved in the magnet hot deformed from the 490 °C high-pressure hot-pressed precursor.

Keywords Nd–Fe–B magnets; Amorphous precursors; Pre-crystallized grains; Hot deformation; Microstructure

W. Zhao, Y. Liu, J. Li*, R.-Q. Wang, Y.-C. Qiu
School of Materials Science and Engineering, Sichuan University, Chengdu 610065, China
e-mail: abthonyli@163.com

J. Li
Key Laboratory of Advanced Special Material and Technology, Ministry of Education, Chengdu 610065, China

1 Introduction

Nd–Fe–B based magnets exhibit outstanding magnetic performance among other commonly used permanent magnets nowadays. They also have wide applications in traction motor for hybrid and pure electric vehicles, speakers of mobile phone [1–5]. Anisotropic Nd–Fe–B magnets can have excellent magnetic properties due to high saturation magnetization of $Nd_2Fe_{14}B$ phase and large magnetocrystalline anisotropy energy [6]. So far, anisotropic Nd–Fe–B magnets are generally manufactured by two different methods: one is sintering, and the other is hot deforming. Hot-deformed anisotropic Nd–Fe–B magnets have attracted much attention because of their excellent magnetic performance together with desirable thermal stability, corrosion resistance and fracture toughness [7, 8]. On the other hand, it has a simpler process than sintering [9, 10]. The texture is formed via a stress-induced preferential grain growth [11, 12], and the alignment of hard magnetic grain (a good texture) is of utmost importance to achieve high performance for the permanent magnet. Traditionally, the hot-deformed anisotropic magnets are produced by two steps: hot press followed by hot deformation. Since the properties of magnetic materials are sensitive to their microstructure, a homogeneous fine grain structure is beneficial to the magnetic properties. Their preparation technique, however, is still a major concern, since their magnetic properties will dramatically deteriorate due to excessive grain growth during the densification and deformation process by conventional method [13, 14]. Based on the above consideration, a more favorable approach should be employed to consolidate the powders into bulk magnets to avoid substantial grain growth for practical application.

It is also worthy noting that the traditional method may cause inhomogeneous microstructure in hot-pressed precursors, thus deteriorating the crystallographic alignment of the $Nd_2Fe_{14}B$ phase in hot-deformed magnets [15]. Up to now, lots of work has been carried out concerning how to obtain a homogeneous microstructure in order to achieve good crystallographic alignment of the $Nd_2Fe_{14}B$ phase [16–18]. It is well known that the most pronounced merit of amorphous materials is their extremely homogeneous microstructure, which was believed as the foundation to obtain a well alignment in hot-deformed magnet. And for this respect, lots of researches were performed with the employment of amorphous powders as starting material. However, most of them were focused on the optimization of process in high-pressure annealing [19–21]. Merely work was conducted to probe the dependence of microstructural evolution during hot deformation process on the precursors with different ratios of crystallization. Moreover, the effects of pre-crystallized grains on microstructure and magnetic properties still remain unclear.

In this work, starting materials with different proportions of amorphous precursors were designed and prepared by hot pressing using spark-plasma sintering (SPS) and then hot-deformed into anisotropic Nd–Fe–B magnets. The influence of different crystallization proportions on microstructure and magnetic properties of the hot-deformed magnets was investigated. Also, it was evaluated the guiding effects of pre-crystallized grains on crystallization and preferential orientation during hot deformation.

2 Experimental

The alloy ingot with a nominal composition of $Nd_{28.72}$ $Fe_{bal}Co_{5.66}Ga_{0.59}B_{0.92}$ (wt%) was prepared by induction melting under an argon atmosphere. The ingot was crushed into small granules and then melt-spun onto a copper wheel rotating at a surface speed of $35~m \cdot s^{-1}$ under an argon atmosphere, and the as-spun flakes were then crushed to 150–200 μm. Then the amorphous powders were consolidated into precursors with different crystallization proportions by spark-plasma sintering (SPS, Dr. Sinter-1050) at various temperatures below the crystallization point in a tungsten carbide mold with a diameter of 10 mm. The conditions of sintering were as follows: The hot-pressing temperature ranged from 450 to 570 °C, the holding time and pressure were 3 min and 1.1 GPa, respectively. Besides, a reference precursor completely crystallized was also prepared by the conventional method (hot pressed at 700 °C).

After the precursors were obtained, hot deformation was carried out to prepare the anisotropic magnets. As the purpose of this study is to reveal the influence of crystallization proportion in precursor on the final magnetic properties, thus the optimal hot deformation condition obtained from our previous study was chosen for magnets preparation in this paper. In this process, an open graphite die (Φ 30 mm) was used for hot deformation conducted at 730 °C in vacuum under the pressure of 15–40 MPa for 2 min with the height reduction of 75%.

The phase constitution of precursors and the degree of crystal alignment of magnets were measured by X-ray diffractometer (XRD, DX-2700) with Cu Kα radiation operated at 30 kV and 40 mA with a scanning rate of 0.03 $(°) \cdot s^{-1}$. The morphology of the grains was analyzed by field emission scanning electron microscope (FESEM, JSM-7500F). A Mossbauer spectrometer (MS-500) was used for the identification of the phase constituents in precursors. Small specimens (Φ 2.5 mm × 2.5 mm) were cut by electric spark linear cutting machine for measurements of magnetic properties, which was done with a vibrating sample magnetometer (VSM, Lake Shore 7410).

3 Results and discussion

3.1 Phase constitution and microstructure of hot-pressed precursors

At first, four hot-pressed precursors with different crystallization proportions were obtained. Figure 1 shows XRD patterns of the hot-pressed precursors obtained at different temperatures along with the as-spun powders. It can be seen that the as-spun powders and the precursor hot-pressed at 450 °C exhibit broad bump curves without any characteristic peaks, indicating amorphous structure of both samples. When hot-pressing temperature reaches 490 °C, some diffraction peaks emerge on the broad
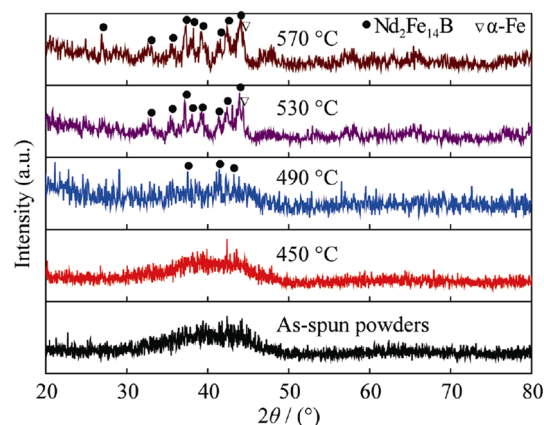

Fig. 1 XRD patterns of as-spun powders and hot-pressed precursors obtained at different temperatures

amorphous diffraction bump, suggesting the formation of nanocrystalline particles at this temperature, namely the beginning of crystallization. For samples prepared at temperatures above 490 °C, the intensity of the crystalline peaks significantly increases and more peaks appear, indicating the increase of crystallization rate. For the hot-pressed isotropic precursors, all the major peaks that appear in XRD patterns could be indexed as the tetragonal hard magnetic $Nd_2Fe_{14}B$ phase, as shown in Fig. 1. From XRD analyses, it can be seen that the crystallization in the precursor starts at 490 °C and develops with the temperatures approaching to crystallization point.

The above results could be further confirmed by SEM images, as shown in Fig. 2. SEM images of precursor hot pressed at 450 °C (Fig. 2a, e) are featureless in both low and high magnifications, indicating its completely amorphous structure. In Fig. 2b, the change of morphology can be clearly noticed in the precursor hot pressed at 490 °C compared with that at 450 °C. Although in the low magnification (Fig. 2b) the crystallization zone could hardly be distinguished, noticeable crystallization strips (labeled by yellow arrow in Fig. 2f) can be found in the high magnification. With the increase of temperature in hot-pressing process, crystallization strips are more noticeable and can be easily observed in the low magnifications as shown in Fig. 2c, d, demonstrating the highly development of the crystallization in the hot-pressed samples. It should be noted that the degree of crystallization could vary a lot from region to region in the same sample, which could be seen from the high-magnified images (Fig. 2g, h) that both highly crystallized region and amorphous region co-exist close to each other with an obvious boundary lying between them. Generally, crystallization would not occur

in the isotropic precursors consolidated below the crystallization temperature. However, in this study, it is found out that under high pressure, crystallization could as well happen even below the crystallization point, clearly demonstrating the promotion effect of high pressure on crystallization. The similar promotion effect of high pressure was also mentioned in some previous studies [22, 23]. Specifically, in Ref. [23], it was pointed out based on an analysis of crystallization kinetics that the high pressure could promote the nucleation rate of nanocrystals in amorphous alloys.

At the same time, the size of pre-crystallized grains formed during hot-pressing process increases with the elevation of hot-pressing temperature (Fig. 2f, g, h). Such discrepancy of grain size in hot-pressed precursors would considerably influence the development of the crystallographic texture in hot-deformed magnets. In fact, previous study has pointed out that high pressure would suppress the grain growth during fabrication in general [22]. And the equation given by Refs [24, 25] could also support this point of view:

$$\left(\frac{\partial \ln D}{\partial p}\right)_T = -\frac{V^*}{k_B T} \tag{1}$$

where p, D, V^*, T and k_B represents the pressure, the diffusion coefficient, the activation volume, the absolute temperature and the Boltzmann's constant, respectively. Normally, the activation volume (V^*) for atom diffusion in amorphous alloys is positive [25]; therefore, the atomic diffusion coefficient (D) decreases with pressure. As a result, the grain growth of the high-pressure-induced nanocrystals could be, on the contrary, constrained by high pressure. Therefore, the combination of the easy nucleation
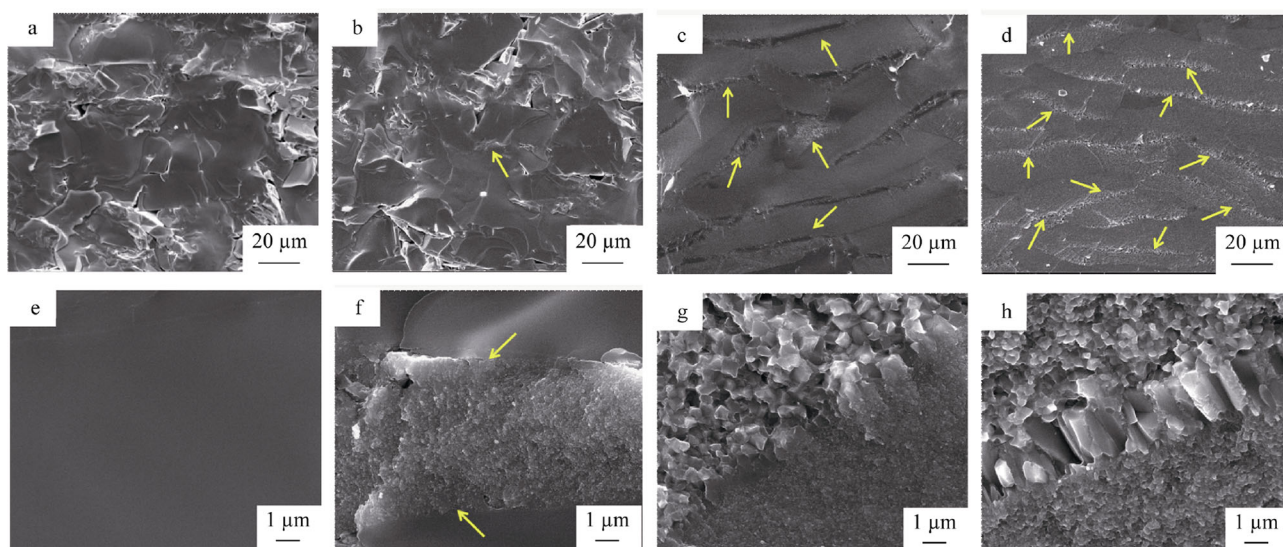

Fig. 2 SEM images of hot-pressed precursors obtained at different temperatures: **a**, **e** 450 °C, **b**, **f** 490 °C, **c**, **g** 530 °C, and **d**, **h** 570 °C (arrows in **b**, **c**, **d** and **f** pointing to clusters of crystallization zone)

and constrained growth behavior promotes the formation of a fine and homogeneous microstructure. However, when the temperature is high, it is hard to avoid the abnormal growth which happens during the hot-pressing process. With the variation of the temperature, more and more grains possess enough energy that allow them surpass the energy barrier of grain growth. Under this circumstance, some grains grow with the temperature variation inevitably. In summary, these changes of morphology verify the crystallization occurred during the high-pressure hot-pressing process, and the crystallization rate increases with the increase of the temperature.

The accurate quantification of crystallization proportion was determined according to the Mossbauer spectra (Fig. 3). It can be seen that the relative intensity of $Nd_2Fe_{14}B$ contributions increases with the increase of temperature. The Mossbauer spectra of hot-pressed precursors obtained at 450 °C show a broadening of the six sextet absorption lines, indicating completely amorphous structure. Furthermore, the calculated spectra area ratio is approximately 0%, 18.9%, 58.4% and 82.2%, corresponding to $Nd_2Fe_{14}B$ phase in hot-pressed sample treated at 450, 490, 530 and 570 °C, respectively. The Mossbauer results suggest that the content of $Nd_2Fe_{14}B$ phase

increases steadily with temperature rising, providing evidently proof to that the crystallization could take place under high pressure even below the crystallization point. Furthermore, it is noticeable that the content of $Nd_2Fe_{14}B$ phase is very high in the sample hot pressed at 570 °C, which implies that high pressure could efficiently reduce the crystallization temperature for amorphous alloys.

3.2 Microstructure and magnetic properties of hot-deformed magnets

Four hot-pressed precursors with crystallization proportions of approximately 0%, 18.9%, 58.4% and 82.2% were obtained along with a completely (100%) crystallized one made by conventional method above crystallization temperature. For the purpose of investigating the effects of crystallization ratio in precursor on the microstructure and magnetic performance in the anisotropic magnet, the same optimal hot deformation condition was used to prepare all the magnets. During the hot-deforming process, the precursors were subjected to a pressure, which would result in anisotropic magnets with the c-axis alignment parallel to the press direction. There are two main kinds of internal microscopic processes in the hot deformation process. One
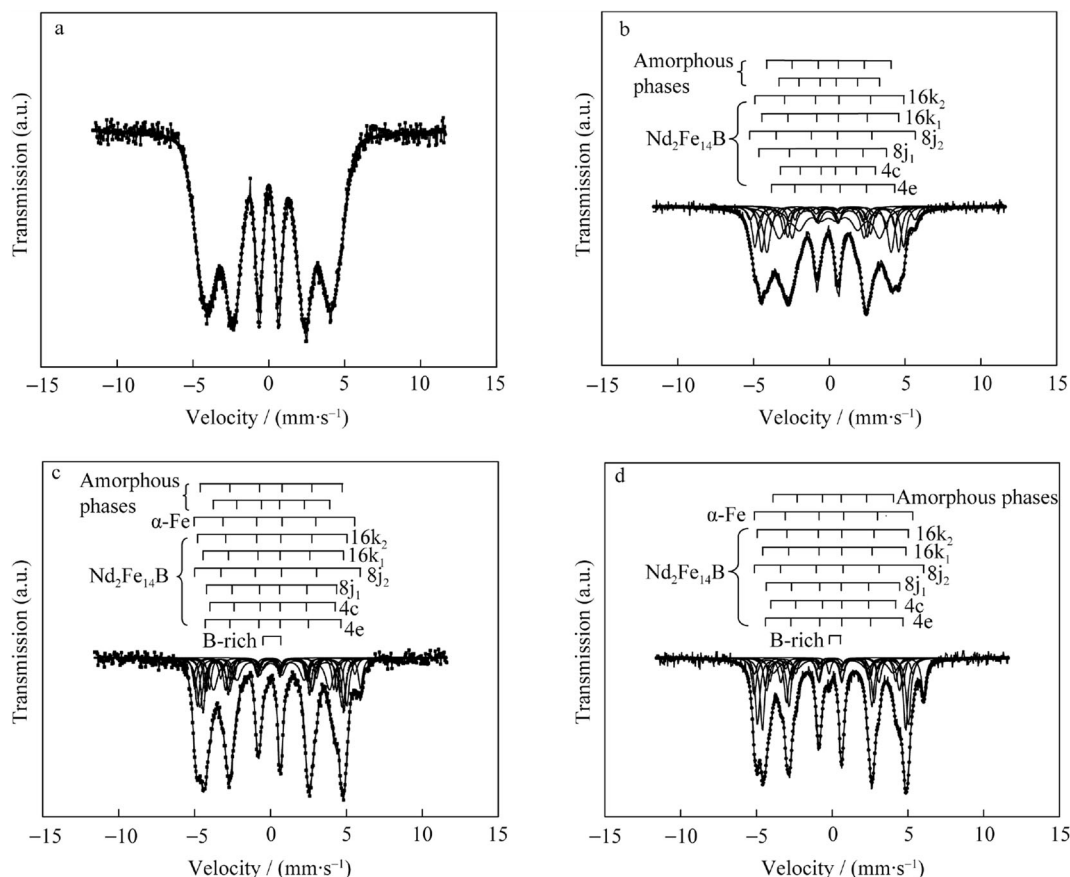

Fig. 3 Mossbauer spectra of hot-pressed precursors obtained at different temperatures: **a** 450 °C, **b** 490 °C, **c** 530 °C, and **d** 570 °C

is the crystallization of the un-crystalized amorphous grains in the hot-pressed precursor. The other is the development of the texture. As it was recognized in previous study, the elastic modulus of the $Nd_2Fe_{14}B$ grain along its easy magnetization axis (*c*-axis) is smaller than that along the hard magnetization axis. Therefore, the grain with its *c*-axis parallel to the pressing direction (favorable grain) has lower total energy compared to the grain with its *c*-axis out of the pressing direction (unfavorable grain) [26]. Under this circumstance, those unfavorable pre-crystallized grains are more likely to dissolve into the Nd-rich liquid phase due to their higher energy. Thus, the unfavorable pre-crystallized grains diminish and the favorable ones become predominant and grow laterally to form platelet grains. The platelet pre-crystallized favorable grains have their easy magnetization axis (*c*-axis) parallel to the pressing direction, leading to a textured grain structure, and subsequently, post-crystallized grains inherit a crystallographic relationship from deformed grains under pressure.

This explanation for the texture formation can be further verified by observing microstructure of the hot-deformed samples. Figure 4 shows the microstructure of the hot-deformed samples prepared from hot-pressed precursors with different crystallization proportions. As can be seen, the grain morphology in hot-deformed samples has significant difference from that in hot-pressed precursors shown in Fig. 2. It appears that the grains are no longer equiaxial shaped; instead, the grains are in elongated shape. The long axis of the elongated grain is perpendicular to the pressing direction (as shown by white arrow in Fig. 4). This observation indicates that the change of grain morphology and the textural development during hot-deforming process takes place by stress-induced preferential grain growth via dissolution and precipitation mechanism [26]. Considering the texture formation mechanism, pre-crystallized grains in hot-pressed precursors play an important role in hot deformation process and are beneficial for the enhancement of the *c*-axial texture parallel to the press direction. Besides, owing to the existence of the pre-crystallized grains, a better-orientated texture could be obtained with the precursor containing a suitable proportion of pre-crystallized grains.

The grain alignment parallel to the press direction of the hot-deformed samples was measured using XRD, as shown in Fig. 5. A good texture is represented by clear (00*l*, *l* = 4, 6, 8) peaks combined with a weak (105) peak. The degree of grain texture can be estimated by the ratio of the peak intensity of the (006) and (105) [27]. From XRD patterns in Fig. 5, it is observed that the peaks such as (004), (006), (105) and (008) become dominant in all hot-deformed magnets, indicating the marked *c*-axis crystallographic alignment in the magnets. The intensities of
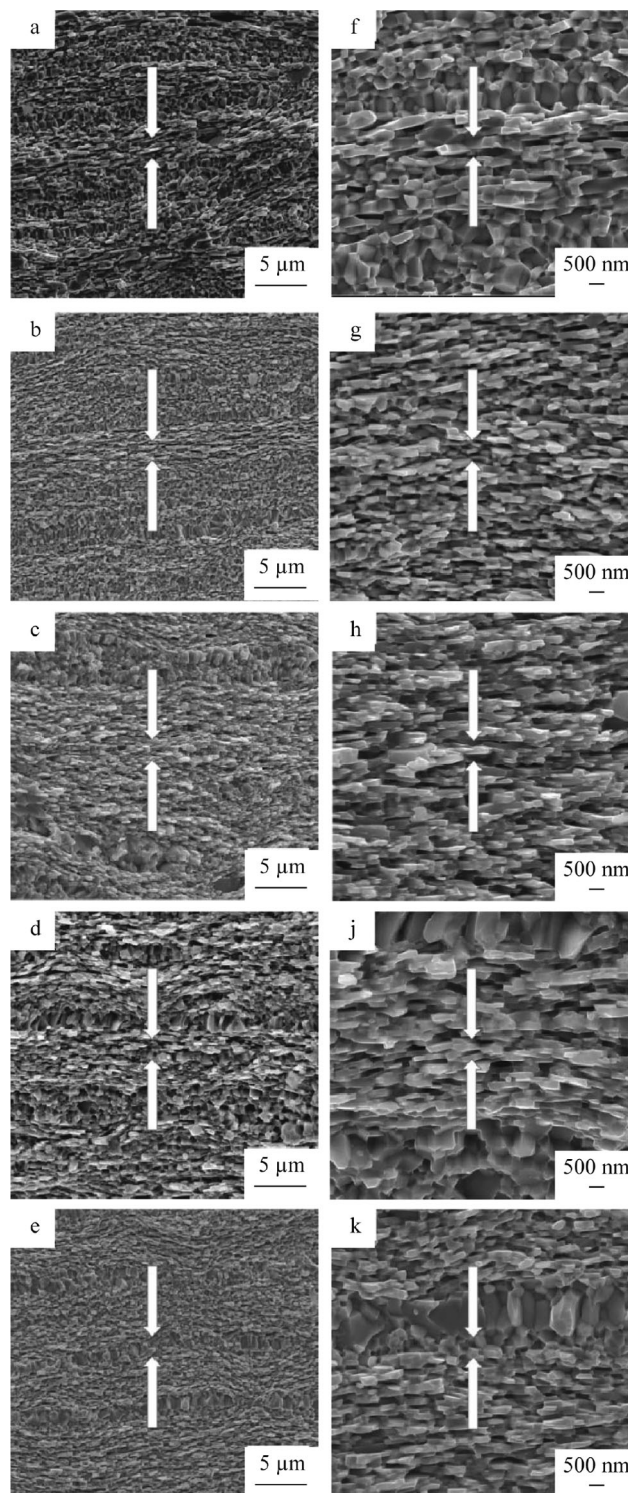
Fig. 4 SEM images of hot-deformed magnets prepared from hot-pressed precursors treated at temperatures **a, f** 450 °C, **b, g** 490 °C, **c, h** 530 °C, **d, j** 570 °C, and **e, k** prepared by conventional method (white arrows indicating pressing direction)

(006) and (105) peaks of the hot-deformed magnets increase sharply compared with those of hot-pressed precursors Fig. 1), indicating the development of a strong
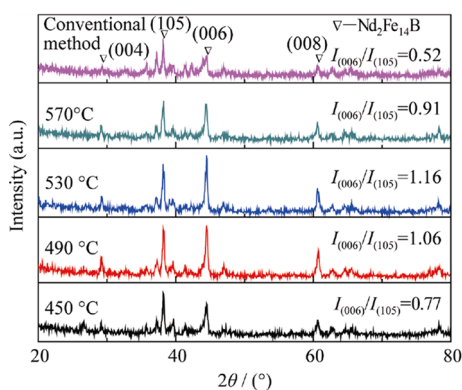
Fig. 5 XRD patterns of hot-deformed magnets prepared from hot-pressed precursors treated at various temperatures and prepared by conventional method

texture along press direction. The results show a better grain alignment in the hot-deformed magnets prepared from hot-pressed amorphous grain containing precursors than the one prepared by conventional method.

The peak intensity of (006) gradually increases with the rise of crystallization degree at first while slightly decreases in the end. And the calculated results of the intensity ratio of (006)/(005) ($I_{(006)}/I_{(005)}$) are shown in Fig. 5, illustrating that it as well increases firstly and then decreases. In other words, the crystallographic texture in the magnets produced from a small proportion crystallization precursor is better than that produced from a large proportion crystallization one, which could be ascribed to the suitable amount of the pre-crystallized grains. The existence of a small amount of pre-crystallized grains is beneficial to the nucleation as well as the growth of the hard magnetic phase during hot deformation process for they are relatively more active and of the biggest surface areas which offer abundant nucleation sites for $Nd_2Fe_{14}B$ phase. And those large numbers of nucleation sites are the sources of tiny dispersive grains to be formed in latter process, which means that much more grains with smaller particle size would form in one unit volume in the same condition. This would do a great favor to the development of grain texture in deformation process. Meanwhile, it is quite possible that the pre-crystallized grains are deformed first during deformation process, and subsequently, post-crystallized grains inherit a crystallographic alignment from the deformed grains under pressure. Considering the textural development mechanism, two main kinds of process could be summarized as follows; one is through grain-boundary sliding, and the other is the process of solution-precipitation creep. Owing to the existence of the pre-crystallized grains, preferred orientation could be realized in them in priority through grain-boundary sliding under a pressure. And then the post-crystallized grains can promptly achieve the grain alignment following the pre-

crystallized ones; meanwhile, large population of pre-crystallized grains might grow quickly due to the excess heat during hot-deforming process. As a result, the presence of large grains zone is observed, which is detrimental to the alignment of the grains. Therefore, a better grain alignment is found in the magnets prepared from a partially crystallized precursor than a completely crystallized one. Hence, taking the two aspects into account, a good grain alignment could be achieved via hot deformation using a hot-pressed precursor with a small proportion of pre-crystallized grains.

From the microstructure of the anisotropic magnets shown in Fig. 4, this partial crystallization advantage could be further confirmed. The grain of hot-deformed magnets is elongated perpendicularly to the press direction and platelet-shaped, indicating the desired crystalline texture formed and developed after hot deforming. It could be observed in Fig. 4f that the microstructure of the fine grain zones consists of small platelet-shaped $Nd_2Fe_{14}B$ grains, which could be ascribed to the deformation of the grains in the process. For the hot-deformed magnets prepared from hot-pressed precursors with large proportion of crystallization and the one prepared by conventional method, there is a large amount of area consisting of the round and equiaxed grains, which is a distinct sign of poor developed texture in those hot-deformed alloys. Beyond that, in the coarse grain zones, as shown in Fig. 4j, k, however, the equiaxed grains are even remained, which could be resulted from the difficulty in deforming the large grains formed during hot-pressing process. Furthermore, the fine grains need a shorter diffusion distance for preferential growth of $Nd_2Fe_{14}B$ grain and a high driving force exists for growth of small grains compared to the large grains [28]. In the hot deformation process, the shape of the finer grains would change from equiaxial spheroid to arrays of plate-like grains with a good crystallographic texture. The mechanism for this texture development has been discussed previously. It can be seen clearly that the grain size reaches the minimum value when hot-pressed temperature is 490 °C and the alignment of grains could also exhibit the best preferential orientation simultaneously. In contrast, with the increase of the crystallization proportion, the grain size sharply increases, while the orientation of the coarser grains keeps the same. This indicates that the texture in the hot-deformed magnets deteriorates with grain growth in the hot-pressed precursor, which is rather unfavorable to the magnetic properties. Thus, the hot-deformed magnets prepared from a hot-pressed precursor with large crystallization proportion could not obtain an excellent grain texture due to the grain growth during hot press process.

Considering the textural formation mechanism discussed earlier in this study, it could be readily understood the effects of grain size in hot-pressed precursor on the

texture in the hot-deformed magnet. Large grain size in the hot-pressed precursor would cause the incomplete dissolution of the unfavorable large grains in the short period of hot deformation process. And the remaining of the undissolved large grains would further hinder the deformation process and prevent the magnet, achieving a better preferential orientation texture. Therefore, the higher crystallization proportion in the hot-pressed precursor would finally lead to unsatisfactory magnetic performance in hot-deformed magnet.

The magnetic properties were investigated by preparing samples cut from the hot-deformed cylinder. The demagnetization curves and the variation of the coercivity (H_{ci}), remanence (B_r), and maximum energy product [$(BH)_{max}$] of the hot-deformed magnets are shown in Figs. 6 and 7. With the increase of the crystallization proportion, the remanence gradually increases from 1.25 to 1.33 T, whereas in the highest crystallization proportion magnet, B_r decreases instead. Furthermore, as for the coercivity, it drastically decreases when hot-pressing temperature exceeds 490 °C, achieving the maximum value of 1187 kA·m^{-1} at 490 °C. The value of $(BH)_{max}$ in a magnet is roughly positive correlated to its B_r. Therefore, $(BH)_{max}$ in anisotropic magnets prepared in the present study increases with temperature rising first, reaches its maximum value of 271 kJ·m^{-3} at 490 °C and then drastically decreases. In addition, it is found that the magnetic properties of magnets prepared from a partial crystallized precursor are better than the one produced by conventional method ($B_r = 1.21$ T, $H_{ci} = 947$ kA·m^{-1}, and $(BH)_{max} = 244$ kJ·m^{-3}), in which the completely crystallized grains show larger particle size in general. This result further corroborates the positive effects of grain refinement and alignment in magnet.

The increase of B_r in anisotropic magnets with the increase of crystallization proportion results from an increasing degree of grain texture. This is related to the
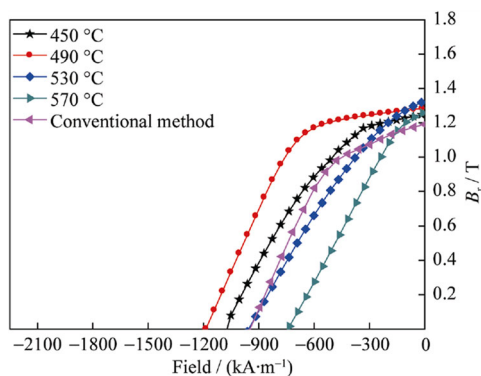

Fig. 6 Demagnetization curves of hot-deformed magnets prepared from hot-pressed precursors treated at various temperatures and prepared by conventional method
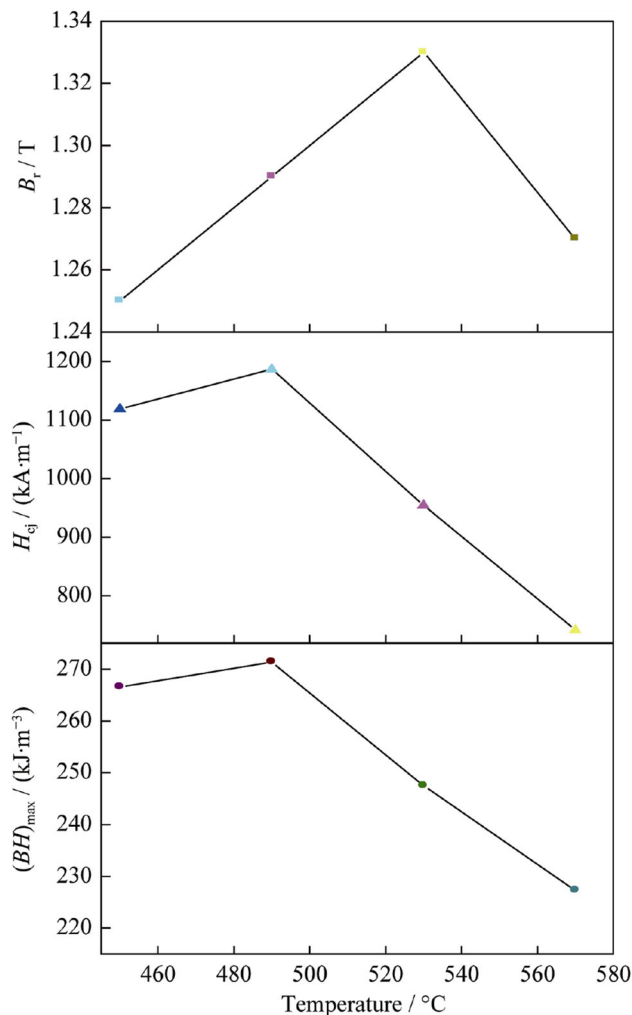

Fig. 7 Effect of crystallization proportion on remanence, intrinsic coercivity and energy product of hot-deformed magnets

existence of the pre-crystallized grains in the isotropic precursors, which may promote the c-axis crystallographic texture. The results could be confirmed by XRD patterns of hot-deformed magnets in Fig. 5. The rapid decrease of coercivity in anisotropic magnets with hot-pressing temperature above 490 °C results from the abnormal grain growth during hot deformation process. The grain growth takes place already during the densification of precursor and keeps proceeding during hot deformation process. There is a particular tendency for growth of the grains located at and near the boundaries between the sintered powder particles. The relation between grain size and H_{ci} has been discussed elsewhere [29–31]. The value of $(BH)_{max}$ in anisotropic magnets is originally proportional to the value of its B_r. Therefore, both $(BH)_{max}$ and B_r of anisotropic magnets prepared in this study increase with a developing degree of grain texture at first, nevertheless then sharply decrease due to the repaid growth of the grain size.

The anisotropic magnet with optimal magnetic performance was prepared from the precursor with $\sim 18.9\%$ crystallization proportion among all the samples, which shows magnetic properties of $B_r = 1.29$ T, $H_{ci} = 1187$ kA·m^{-1} and $(BH)_{max} = 271$ kJ·m^{-3} under the best process condition.

4 Conclusion

Anisotropic magnets were prepared by hot-deforming hot-pressed precursors with different crystallization proportions. The study reveals that the final obtained magnet shows a strong magnetic performance depending on the crystallization proportion in precursors. With the crystallization proportion of ~ 18.9 vol% in precursor, the magnet exhibits the optimal properties of $B_r = 1.29$ T, $H_{ci} = 1187$ kA·m^{-1} and $(BH)_{max} = 271$ kJ·m^{-3} among all the samples. Besides the influences of crystallization proportion of precursor on the microstructure and magnetic properties of the hot-deformed magnet, the function of pre-crystallized grains in the hot-deforming process was also investigated. It is found that the pre-crystallized grains show a guiding effect in the hot-deforming process that leads to the alignment inheriting of post-crystallized grain from the pre-crystallized ones. Accordingly, a suitable amount of pre-crystallized grains containing precursor would be much favorable to prepare a high-performance hot-deformed magnet. The hot-deformed magnet would fail to achieve the optimal magnetic properties with neither too little nor too much pre-crystallized grains in the precursor. The precursor hot pressed at 490 °C acquires the most suitable amount of crystallization proportion, from which the magnet prepared shows a good crystallographic alignment parallel to the pressing direction. Additionally, hot-deformed magnet prepared from partial crystallized precursor exhibits a better crystallographic alignment and finer grain size compared with the one prepared by conventional method. This result shows a novel way and an opportunity to prepare bulk nanocomposites with homogeneous microstructure and enhanced magnetic properties from partial crystallized precursors, which therefore might be of wide interest.

References

[1] Yu YP, Liu Y, Li J, Zheng Q, Wang RQ. Desorption-recombination behavior of as-disproportionated NdFeCoB compacts by reactive deformation. Rare Met. 2015;34(2):89.

[2] Li YF, Zhu GM, Li AH, Feng HB, Huang SL, Li W, Du A, Qi Y. Relationship between controllable preparation and microstructure of NdFeB sintered magnets. J Rare Earth. 2014;32(7):628.

[3] Sugimoto S. Current status and recent topics of rare-earth permanent magnets. J Phys D Appl Phys. 2011;44(6):064001.

[4] Hadjipanayis GC, Liu JF, Gabay A, Marinescu M. Current status of rare-earth permanent magnet research in USA. J Iron Steel Res Int. 2006;13(S1):12.

[5] Skomski R, Sellmyer DJ. Anisotropy of rare-earth magnets. J Rare Earth. 2009;27(4):675.

[6] Zheng Q, Li J, Liu Y, Yu YP, Lian LX. Highly oriented NdFeCoB nanocrystalline magnets from partially disproportionated compacts by reactive deformation under low pressure. J Appl Phys. 2014;115(17):173511.

[7] Hou YH, Huang YL, Liu ZW, Zeng DC, Ma SC, Zhong ZC. Hot deformed anisotropic nanocrystalline NdFeB based magnets prepared from spark plasma sintered melt spun powders. Mater Sci Eng B Adv. 2013;178(15):990.

[8] Ma BM, Lee D, Smith B, Gaiffi S, Owens B, Bie H, Warren GW. Comparison of the corrosion behavior of die-upset and sintered NdFeB magnets. IEEE Trans Magn. 2001;37(4):2477.

[9] Brown D, Ma BM, Chen ZM. Developments in the processing and properties of Nd–Fe–B-type permanent magnets. J Magn Magn Mater. 2002;248(3):432.

[10] Wang XC, Zhu MG, Li W, Li YF, Lai B, Du A. Microstructure and magnetic properties of anisotropic hot-deformed magnet of different magnetic particle sizes. Rare Met. 2015;34(4):255.

[11] Li L, Graham CD Jr. Mechanism of texture formation by hot deformation in rapidly quenched FeNdB. J Appl Phys. 1990;67(9):4756.

[12] Li L, Graham CD. The origin of crystallographic texture produced during hot deformation in rapidly-quenched NdFeB permanent magnets. IEEE Trans Magn. 1992;28(5):2130.

[13] Liu WQ, Cui ZZ, Yi XF, Yue M, Jiang YB, Zhang DT, Zhang JX, Liu XB. Structure and magnetic properties of magnetically isotropic and anisotropic Nd–Fe–B permanent magnets prepared by spark plasma sintering technology. J Appl Phys. 2010;107(9):09A719.

[14] Lin M, Wang HJ, Yi PP, Yan AR. Effects of excessive grain growth on the magnetic and mechanical properties of hot-deformed NdFeB magnets. J Magn Magn Mater. 2010;322(15):2268.

[15] Harada T, Fujita M, Kuji T. Nd-Fe-B die upset magnets produced from amorphous bulk materials. J Alloy Compd. 1996;243(1–2):139.

[16] Lee JI, Kwon HW, Choi GS. Texture in die-upset Nd-Fe–B magnet produced using HDDR-treated particles. Phys Status Solidi c. 2007;4(12):4617.

[17] Wang L, Chen JW, Yue M, Liu RM, Liu WQ. Crystallographic alignment and magnetic anisotropy in melt-spun Nd-Fe-B/α-Fe composite ribbons with different neodymium contents. J Rare Earth. 2011;29(5):471.

[18] Ma YL, Chen DM, Zhou AR, Sun JC, Cao PJ. Enhanced alignment and magnetic properties of die-upset nano-crystal $Nd_2Fe_{14}B$ magnets with Nb addition. Phys B. 2012;407(23):4562.

[19] Li XH, Gao ZS, Li W, Zhang KW, Zhang JW, Zhang XY. Study of the microstructure of α-Fe/$Nd_2Fe_{14}B$ nanocomposites prepared by electropulsing heating amorphous NdFeCoB. Mater Lett. 2005;59(22):2782.

[20] Li W, Li LL, Nan Y, Li XH, Zhang XY. Controllable nanocrystallization in amorphous $Nd_9Fe_{85}B_6$ via combined application of severe plastic deformation and thermal annealing. Appl Phys Lett. 2007;91(6):062509.

[21] Liu YG, Xu L, Guo DF, Li W, Wang QF, Zhang XY. Bulk anisotropic $Nd_2Fe_{14}B$/α-Fe nanocomposite magnets prepared by

hot deformation processing of amorphous alloys. J Appl Phys. 2009;106(11):113918.

[22] Wu W, Li H, Xie YW, Zhang XY. Effect of high pressure on microstructure of crystallizing amorphous $Nd_9Fe_{85}B_6$ alloy. J Rare Earth. 2008;26(5):741.

[23] Liang BY, Xie YW, Li W, Wu W, Zhang XY. Microstructure and magnetic properties of bulk nanocomposite magnets prepared by crystallizing amorphous $Nd_{3.6}Pr_{5.4}Fe_{80}Co_3B_7Nb_1$ under high pressure. J Phys D Appl Phys. 2008;41(19):195010.

[24] Wu W, Li W, Sun HY, Li H, Li XH, Liu BT, Zhang XY. Pressure-induced preferential growth of nanocrystals in amorphous $Nd_9Fe_{85}B_6$. Nanotechnology. 2008;19(28):285603.

[25] Faupel F, Frank W, Macht MP, Mehrer H, Naundorf V, Raetzke K, Schober HR, Sharma SK, Teichler H. Diffusion in metallic glasses and supercooled melts. Rev Mod Phys. 2003;75(1):237.

[26] Kwon HW, Kang YS, Choi GS, Yu JH. Effect of grain size and die-upset temperature on texture in die-upset Nd-Fe-B magnet. IEEE Trans Magn. 2009;45(6):2590.

[27] Lee YI, Shih CW, Chang WC, Chang HW, Chen YJ. Inhomogeneity on texture, microstructure and magnetic properties of hot deformed $R_2Fe_{14}B$-typed magnet. Int J Mod Phys B. 2015; 29(10):154007.

[28] Lipiec W, Davies HA. The influence of the powder densification temperature on the microstructure and magnetic properties of anisotropic NdFeB magnets aligned by hot deformation. J Alloy Compd. 2010;491(1–2):694.

[29] Sun Y, Gao RW, Feng WC, Han GB, Bai G, Liu T. Effect of grain size and distribution on the anisotropy and coercivity of nanocrystalline $Nd_2Fe_{14}B$ magnets. J Magn Magn Mater. 2006; 306(1):108.

[30] Feng WC, Gao RW, Yan SS, Li W, Zhu MG. Effects of phase distribution and grain size on the effective anisotropy and coercivity of nanocomposite $Nd_2Fe_{14}B/\alpha$-Fe magnets. J Appl Phys. 2005;98(4):044305.

[31] Fischer R, Schrefl T, Kronmfiller H, Fidler J. Grain-size dependence of remanence and coercive field of isotropic nanocrystalline composite permanent magnets. J Magn Magn Mater. 1996;153(1–2):35.